ON THE LARGE-SCALE DIFFUSE MAGNETIC FIELD OF THE SUN

MAUSUMI DIKPATI
Department of Physics, Indian Institute of Science, Bangalore 560012, India; and Indian Institute of Astrophysics, Bangalore 560034, India

and

ARNAB RAI CHOUDHURI
Department of Physics, Indian Institute of Science, Bangalore 560012, India; and Kiepenheuer-Institut für Sonnenphysik, D-79104, Freiburg, Germany

(Received 12 December, 1994)

Abstract. Although the sunspots migrate towards the equator, the large-scale weak diffuse magnetic fields of the Sun migrate poleward with the solar cycle, the polar field reversing at the time of the sunspot maxima. We apply the vector model of Dikpati and Choudhuri (1994, Paper I) to fit these observations. The dynamo layer at the base of the convection zone is taken to be the source of the diffuse field, which is then evolved in the convection zone subject to meridional circulation and turbulent diffusion. We find that the longitudinally averaged observational data can be fitted reasonably well both for positive and negative values of the α-effect by adjusting the subsurface meridional flow suitably. The model will be extended in a future paper to include the decay of active regions as an extra source of the diffuse field, which may be necessary to explain the probable phase lag between B_r and B_ϕ at lower latitudes.

1. Introduction

Although the sunspots migrate towards the equator with the progress of the solar cycle, the weak diffuse magnetic fields on the solar surface have been found to migrate poleward (Bumba and Howard, 1965; Howard and LaBonte, 1981; Makarov, Fatianov, and Sivaraman, 1983; Makarov and Sivaraman, 1989; Wang, Nash, and Sheeley, 1989a, b). In a previous paper (Dikpati and Choudhuri, 1991; hereafter Paper I), we have developed a model of this poleward migration of the weak diffuse fields. We wish to present detailed comparisons between our model and the observational data in this paper.

Just as the latitude–time plot of the sunspot number data gives rise to the well-known butterfly diagram, a similar latitude–time plot of the longitude-averaged photospheric field strength at the higher latitudes gives rise to what we call a *reverse butterfly diagram* (see Wang, Nash, and Sheeley, 1989a). The wings of the butterfly are tilted in the reverse direction for this plot, because the fields are migrating to the higher latitude. Figure 1 shows a superposition of these two plots (butterfly and reverse butterfly diagrams) for the same period from May 1976 to December 1985, i.e., we plot both the sunspot data (kindly provided by Dr R. Howard) and the WSO (Wilcox Solar Observatory) data of longitudinally averaged photospheric field strength (kindly provided by Dr Y.-M. Wang) in the same time–latitude graph. Figure 1 shows that the polar field reverses its direction at the time of sunspot

Solar Physics **161:** 9–27, 1995.

maximum (first discovered by Babcock, 1959), clearly implying that there is a phase relation between the sunspot number and the weak diffuse field. One of the aims of this paper is to reproduce Figure 1 theoretically.

In Paper I, we have referred to the magnetic fields of the sunspots as the *toroidal component* of the solar magnetic field, because the sunspots are produced due to the magnetic buoyancy of the toroidal component of the dynamo-generated magnetic field (Choudhuri, 1989; Fan, Fisher, and DeLuca, 1993; D'Silva and Choudhuri, 1993; Caligari, Moreno-Insertis, and Schüssler, 1994). It should, however, be kept in mind that the magnetic field inside a rising flux tube is no longer purely *toroidal* after it has come out of the dynamo layer. On the other hand, Paper I referred to the weak diffuse field as the *poloidal component*, since its evolution is studied in the poloidal plane. It has been pointed out by some of the readers of Paper I that the terms *toroidal* and *poloidal* used in Paper I in this fashion produced considerable confusion and misunderstanding. Hence we shall use the terms *concentrated component* and *diffuse component* instead of *toroidal component* and *poloidal component*.

The ultimate source of the solar magnetic fields is believed to be a dynamo operating in the overshoot layer underneath the convection zone (see Choudhuri, 1990, and references therein). There are reasons to expect that the magnetic field in the dynamo layer is already concentrated to values well above the equipartition value (Schüssler, 1993). It is even conceivable that the instability of the concentrated flux tubes drives the dynamo (Ferriz-Mas, Schmitt, and Schüssler, 1994). Since our understanding of the solar dynamo is still so primitive, it is difficult to say much about the nature of the magnetic field produced in the dynamo layer. If the dynamo is of $\alpha^2\omega$ type as suggested in some recent calculations (Choudhuri, 1990, 1992a), then non-negligible amounts of poloidal field should be produced in addition to the toroidal field. Probably the resulting magnetic field already consists of some concentrated flux tubes and some diffuse field. Since diffusion has always been regarded as an important ingredient of the dynamo process (Moffatt, 1978; Parker, 1979), we expect some diffuse field to be present in and around the dynamo region. Parts of the concentrated flux tubes may rise due to magnetic buoyancy and produce active regions. The decay of active regions can again give rise to some diffuse magnetic field in the surrounding region, as first pointed out by Leighton (1964).

There can thus be two sources of the diffuse magnetic field. It can be produced around the dynamo region, or it can result from the decay of active regions. The NRL group has developed a detailed model of the evolution of the weak diffuse field by assuming the decay of the active regions to be the only source for it (DeVore, Sheeley, and Boris, 1984; Sheeley, DeVore, and Boris, 1985; DeVore and Sheeley, 1987; Sheeley, Wang, and Harvey, 1989; Wang, Nash, and Sheeley, 1989a, b; Wang and Sheeley, 1991). This model treated the magnetic field as a two-dimensional scalar field residing on the solar surface and had some other limitations pointed out in Paper I. We had attempted in Paper I to develop a model incorporating the

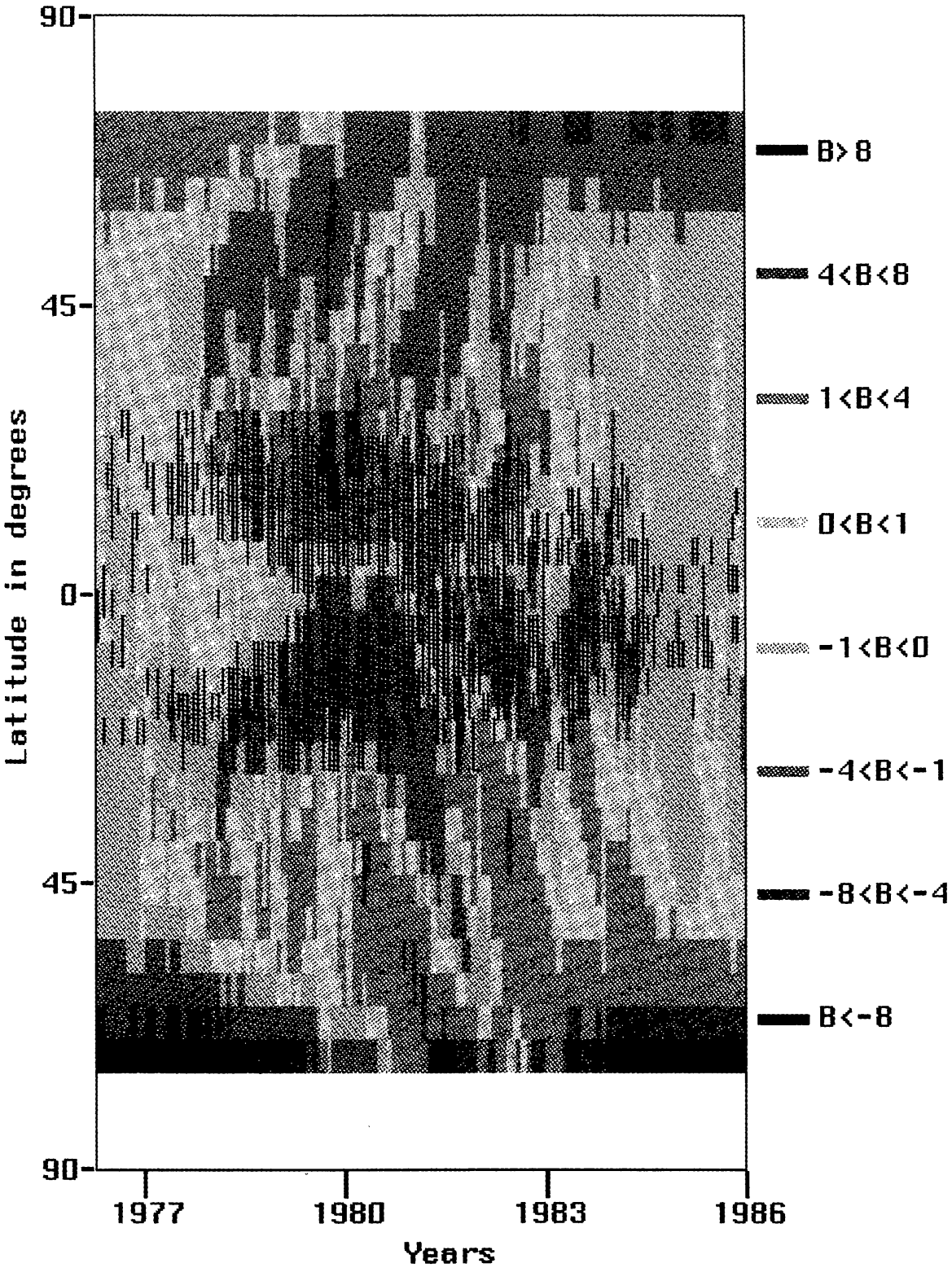

Fig. 1. Colour-shades showing the latitude–time distribution of longitudinally averaged photospheric radial fields (B is in gauss) with a 'butterfly diagram' of sunspots superimposed on it during the interval from May 1976 to December 1985. The colours in the green side of the spectrum represent the negative polarity fields and in the red side represent the positive polarity.

three-dimensional vectorial character of the magnetic field. Our first calculations assumed that the diffuse field produced in the dynamo region is the only source, since it is easier to develop a vectorial model first for this source alone. Our model was fully axisymmetric and hence could not handle the local spread of flux from the active regions which has been successfully modelled by the NRL group. We are now working on an extension of our model which will incorporate both the sources (diffusion in dynamo layer and decay of active regions) of the weak diffuse fields. The present paper, however, explores the feasibility of matching observational data by taking the diffuse field produced in the dynamo region as the only source. It may be noted that Stenflo (1992) has argued on the basis of recent observational data that an appreciable part of the large-scale, diffuse field results from the flux emerging from underneath the surface in the form of ephemeral regions (ER) and intranetwork fields (IN). We believe that it is the diffuse component produced in the dynamo layer, which is ultimately concentrated by the convective motions near the surface and gives rise to the ER and IN. Some authors (Stenflo 1992; Petrovay and Szakály, 1993) have considered the possibility whether this flux could have come up vertically from the dynamo layer. Since magnetic buoyancy is not supposed to be very important for the diffuse component (as we argued in Paper I), we assume that it is passively carried by the meridional circulation and brought to the surface by it.

Our aim is to model the longitude-averaged observational data. By taking the meridional flow velocity and the diffusion coefficient as two completely free parameters which can be chosen to fit the observations, Wang, Nash, and Sheeley (1989a) had shown that their model can fit the data reasonably well. Again by taking the meridional flow and the diffusion coefficient as free parameters, we show that our model can fit the same data equally well and also opens up the possibility of studying the evolution of the corona with the solar cycle. Hence, as long as the meridional flow and the diffusion are regarded as completely free parameters, the two extreme models for the source of the diffuse field (active region decay as the only source or diffusion around the dynamo layer as the only source) can both fit the observational data. We point out that there are some observations on the meridional flow (Komm, Howard, and Harvey, 1993) and the diffusion coefficient (Schrijver and Martin, 1990) on the solar surface, although we know nothing about their values underneath the surface. It is to be noted that both the model of Wang, Nash, and Sheeley (1989a) and our model give best fits with observations for the values of meridional flow on the surface which compare well with the values obtained by very different methods of analysis (Komm, Howard, and Harvey, 1993). If we have tighter constraints on the meridional flow and diffusion in future, it may be possible to ascertain the relative contributions from both the sources. Paper I and this paper should be regarded only as the first steps towards building a full vectorial model of diffuse fields – as opposed to the scalar model of the NRL group. A more complete model with both the sources will be presented in future papers.

As in Paper I, we study the evolution of the large-scale diffuse field in the convection zone as a result of diffusion and meridional circulation. Although the dynamo wave giving rise to this field is propagating equatorward at the base of the convection zone, we show that the field lines in the upper part of the convection zone may be carried poleward by the meridional circulation. After summarizing the basic equations in the next section, we present the results of the calculations in Section 3. The last section discusses the significance of the results.

2. Basic Mathematical Equations

Although the diffuse field may have a component in the toroidal direction also, it is sufficient to concentrate on the poloidal component of the diffuse field alone in order to understand the longitude-averaged (i.e., axisymmetric) evolution of the diffuse field. This can be seen from the following argument. Let us write the axisymmetric magnetic field and velocity field as

$$\mathbf{B} = B_\phi \hat{\mathbf{e}}_\phi + \nabla \times (A\hat{\mathbf{e}}_\phi) \,, \tag{1}$$

$$\mathbf{v} = \mathbf{v}_p + r \sin\theta \omega \hat{\mathbf{e}_\phi} \,, \tag{2}$$

where B_ϕ and A refer to the toroidal and poloidal components of the magnetic field, whereas $\mathbf{v}_p$ and ω refer to the meridional flow and the differential rotation. Substituting (1) and (2) in the induction equation, we find

$$\frac{\partial B_\phi}{\partial t} + s(\mathbf{v}_p \cdot \nabla)\,(s^{-1}B_\phi) = s(\mathbf{B}_p \cdot \nabla)\omega + \eta(\nabla^2 - s^{-2})B_\phi \,, \tag{3}$$

$$\frac{\partial A}{\partial t} + s^{-1}(\mathbf{v}_p \cdot \nabla)\,(sA) = \eta(\nabla^2 - s^{-2})A \,, \tag{4}$$

where $s = r \sin\theta$. We see from (3) that the evolution of the toroidal component may involve the streching of the poloidal field lines by the differential rotation. However, it is clear from (4) that the evolution of the poloidal component does not depend on whether there is also a toroidal component or not. This justifies our studying the poloidal field in isolation in Paper I. In fact, Equation (4) is the basic equation we solved in the spherical geometry in Paper I (it may be noted that Equation (29) in Paper I had some typographical errors). Here also we take the same as our basic equation.

The convection zone is taken to extend from $r = R_b$ to $r = R$. Since the two hemispheres are symmetric, we discuss solutions only in the northern hemisphere (i.e., from $\theta = 0$ to $\theta = \pi/2$). Within this region, we solve (4) subject to similar boundary conditions as in Paper I. An equatorward propagating dynamo wave is taken to provide the bottom boundary condition and acts as the source of the field:

$$A(r = R_b, \theta, t) = \frac{A_0}{[1 + e^{\gamma(\pi/4-\theta)}]} \cos\left[\omega t + kR_b\left(\frac{\pi}{2} - \theta\right)\right] . \quad (5)$$

Here ω is the frequency of the dynamo wave and k is the dynamo wave number. Again γ is taken to be 8.0. From the 22-year periodicity of dynamo wave, ω is found to be 9.1×10^{-9} s^{-1} and a half wavelength of 40° in θ-direction corresponds to $k = 9.2 \times 10^{-11}$ cm^{-1}. The boundary conditions at the pole and the equator are

$$A = 0 \quad \text{at} \quad \theta = 0 , \quad (6)$$

$$\partial A/\partial\theta = 0 \quad \text{at} \quad \theta = \pi/2 . \quad (7)$$

The significances of the three boundary conditions (5), (6), and (7), which are the same as in Paper I, are discussed there.

We treat the upper boundary condition somewhat differently in this paper. In Paper I we assumed a potential field above the photosphere satisfying the equation $(\nabla^2 - s^{-2})A = 0$. This current-free approximation is not valid if the influence of the solar wind is taken into account. Following Altschuler and Newkirk (1969), we take the field to be potential from the photosphere $r = R$ to a distance $r = R_w$, where the field becomes radial due to the stretching of the solar wind. Generally R_w, can be taken somewhere between $2R$ and $3R$ where the kinetic energy density of the solar wind excedes the magnetic energy density there. From the photosphere to $r = R_w$, we now have to take a solution of the form

$$A(R \le r \le R_w, \theta, t) = \sum_n \frac{a_n(t)}{r^{n+1}} P_n^1(\cos\theta)\left[c_n + (1 - c_n)\left(\frac{r}{R}\right)^{2n+1}\right] , \quad (8)$$

instead of Equation (33) of Paper I. Here $P_n^1(\cos\theta)$ is the associated Legendre's polynomial and the summation is again over all the odd values of n. The coefficients c_n's are found by demanding that

$$B_\theta = 0 \quad \text{at} \quad r = R_w ,$$

which gives

$$\frac{1}{c_n} = 1 + \frac{n}{n+1}\left(\frac{R}{R_w}\right)^{2n+1} . \quad (9)$$

Now instead of (35) in Paper I, we have to match the derivative at the solar surface given by

$$\left.\frac{\partial A}{\partial r}\right|_{r=R} = -\sum_n \frac{(n+1)a_n(t)}{R^{n+2}} P_n^1(\cos\theta)\left[c_n - \frac{n}{n+1}(1 - c_n)\right] . \quad (10)$$

Hence the solution inside the convection zone has to match (8) at the upper surface with the derivative matching (10). Paper I discusses in detail how such boundary conditions can be handled numerically.

With all the boundary conditions specified as above, we can study the evolution of the magnetic field by solving (4), provided the meridional circulation $\mathbf{v}_p$ inside the convection zone is given. Here we prefer to take an expression different from that (van Ballegooijen and Choudhuri, 1988) used in Paper I. The reasons will be clear in the next section. For a compressible flow inside the convection zone, $\nabla \cdot (\rho \mathbf{v}_p) = 0$ is satisfied by taking $\rho \mathbf{v}_p = \nabla \times (\psi \hat{\mathbf{e}}_\phi)$, where ψ is given by

$$\psi r \sin\theta = \psi_0 \sin\left[\frac{\pi(r - R_b)}{(R - R_b)}\right] \{1 - e^{-\beta_1 r \theta^\epsilon}\} \{1 - e^{\beta_2 r(\theta - \pi/2)}\} e^{-((r-r_0)/\Gamma)^2} . \tag{11}$$

Here ψ_0 is a prefactor to determine the maximum speed of the flow and β_1, β_2, ϵ, Γ, r_0 are parameters: β_1 and β_2 control how much concentrated the flow will be at the pole and the equator respectively; ϵ is made slightly greater than 2 to keep the flow nonsingular at the pole. Because of the density stratification of the form (van Ballegooijen and Choudhuri, 1988)

$$\rho(r) = C \left(\frac{R}{r} - 1\right)^m , \tag{12}$$

the flow is expected to circulate through a larger area at the top than at the bottom of the convection zone. The gaussian factor in (7) takes care of this fact. The two velocity components are given by

$$v_r = \frac{1}{\rho r^2 \sin\theta} \frac{\partial}{\partial \theta} (\psi r \sin\theta) , \tag{13a}$$

$$v_\theta = -\frac{1}{\rho r \sin\theta} \frac{\partial}{\partial r} (\psi r \sin\theta) , \tag{13b}$$

whereas the streamlines of flow can be obtained by plotting the contours of constant $\psi r \sin\theta$.

We use the Alternating Direction Implicit (ADI) scheme to solve the partial differential equation (4) with the boundary conditions and the circulation velocity as discussed above. The details of the numerical technique have been discussed in the Appendix of Paper I. The simulated poloidal field lines are obtained by plotting the contours of constant $Ar \sin\theta$ in the meridional plane. To obtain the theoretical 'reverse butterfly diagram', the radial field $B_r = (r^2 \sin\theta)^{-1} \partial/\partial\theta \, (Ar \sin\theta)$ is evaluated at the surface at different times, and then the resulting contours have been plotted in a latitude–time diagram.

The theoretical 'butterfly diagram' can be obtained only when we know the distribution of the toroidal component of the dynamo-generated magnetic field in

the dynamo layer. Since dynamo calculations always show a phase relation between the toroidal and poloidal components, the toroidal component in the middle of the dynamo layer can be written as

$$B_\phi(\theta, t) = \frac{B_0}{[1 + e^{\gamma((\pi/4)-\theta)}]} \cos\left[\omega t + kR_b\left(\frac{\pi}{2} - \theta\right) + \delta\right] , \tag{14}$$

where we have introduced a phase difference δ with respect to Equation (5) for A in the dynamo layer. The Appendix gives a derivation of this phase difference δ for a plane $\alpha^2\omega$ dynamo wave. In the $\alpha\omega$ limit, we have $\delta = \pi/4$ if α is positive and $\delta = 5\pi/4$ if α is negative (provided A_0 and B_0 are taken as positive). We have used these values of δ for our theoretical model. In the other extreme limit of the $\alpha^2\omega$ dynamo (the α^2 limit), the phase differs by a small amount $\pi/4$ from the phase for the $\alpha\omega$ limit. Since these values of δ are for a plane dynamo wave, one may have worries whether things will be very different for a dynamo in a thin layer. Recently, Schlichenmaier and Stix (1994) have carried on a thorough study of the phase relationship of the dynamo under different conditions. They find the phase to be fairly stable and to have values almost always close to the values for plane dynamo waves.

A stronger toroidal field is likely to give rise to more sunspots. A question of vital importance is whether the flux tubes, which break away from the dynamo layer, rise radially to produce sunspots at the same latitudes at which they started at the bottom of the convection zone. The Coriolis force is capable of diverting the rising flux tubes to higher latitudes (Choudhuri and Gilman, 1987; Choudhuri, 1989). Most probably, however, the flux tubes rise roughly along the radial direction (D'Silva and Choudhuri, 1993; D'Silva 1993). In that case, a contour plot of $B_\phi(\theta, t)$, as given by Equation (14), in a latitude–time diagram would give the theoretical 'butterfly diagram'. We finally superpose the theoretical 'butterfly' and 'reverse butterfly' diagrams in the same plot and compare with Figure 1.

3. Results

We now present the results with a view to matching the observational data as given in Figure 1. We may note that during the half-cycle presented in Figure 1, the leading polarity in the northern hemisphere was positive, implying that the subsurface toroidal field B_ϕ was negative in the northern hemisphere. Figure 1 shows that the north polar field changed from positive to negative during this half-cycle. Since our calculations are for the northern hemisphere, we have to show that the polar field changes from positive to negative (negative to positive) at the time of the sunspot maximum when the underlying toroidal field B_ϕ is negative (positive).

Since the phase relation between A and B_ϕ depends on the sign of α, we would like to see if the observational data can be fitted better for a certain sign of α.

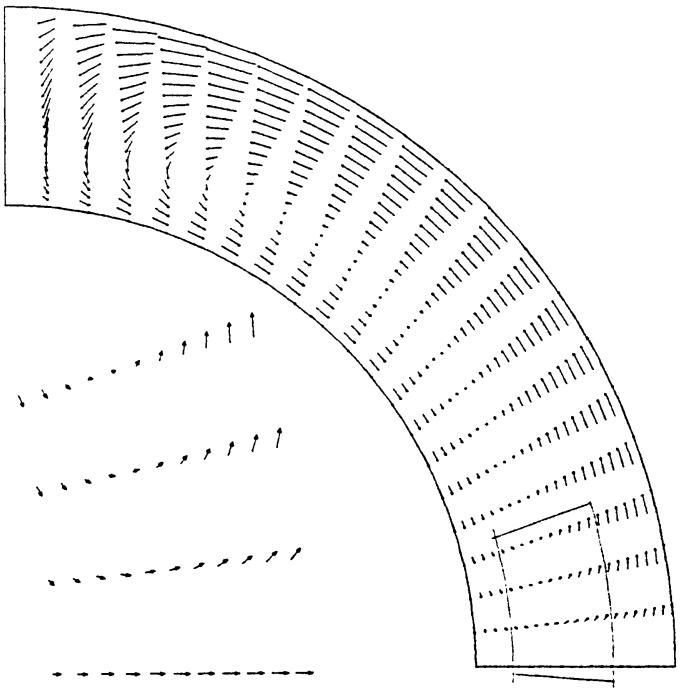

Fig. 2a. The meridional circulation pattern corresponding to the stream function given by (11) with the following values of the parameters: $\beta = 1.5k$, $\beta_2 = k$, $\epsilon = 2.000001$, $r_0 = (R - r_b)/5$, $\Gamma = 3/k$, and $\psi_0 = k^{-1}$. The boxed region is enlarged to show how much concentrated the flow is at the equatorial region.

The sign of α has considerable theoretical significance. The product of α and the velocity shear G has to be negative in the northern hemisphere for the equatorward propagation of the dynamo wave (see Appendix). In the early days of convection zone dynamos, it used to be assumed that α is positive in the northern hemisphere (see Moffatt, 1978, pp. 239–240). Since the helioseismology data show the velocity shear to be positive at the base of the convection zone where the dynamo is now believed to operate, it is now expected that α ought to be negative. Hence any independent argument for the sign of α would be of importance.

We find that the observational data can be fitted for both the signs of α reasonably well if we are free to adjust the meridional circulation according to our needs. Figures 2(a–c) show the fit for positive α. The meridonal flow pattern is shown in Figure 2(a), with the parameters specified in the figure caption. The field lines are plotted in Figure 2(b) for four epochs of time during a half-cycle. The field lines in the positive A regions are shown by solid lines, whereas the field lines in the negative A regions are shown by dashed lines. It is to be noted that the field direction is clockwise in the regions of positive A and anti-clockwise in the regions of negative A. Finally Figure 2(c) presents the superimposed theoretical butterfly diagrams. The contours of B_r are shown by solid lines if B_r is positive and by dashed lines if B_r is negative. The 'butterfly diagrams' obtained from Equation (14) (with $\delta = \pi/4$ for positive α) are shaded with solid lines if B_ϕ is positive and shaded with broken lines if B_ϕ is negative. A comparison of

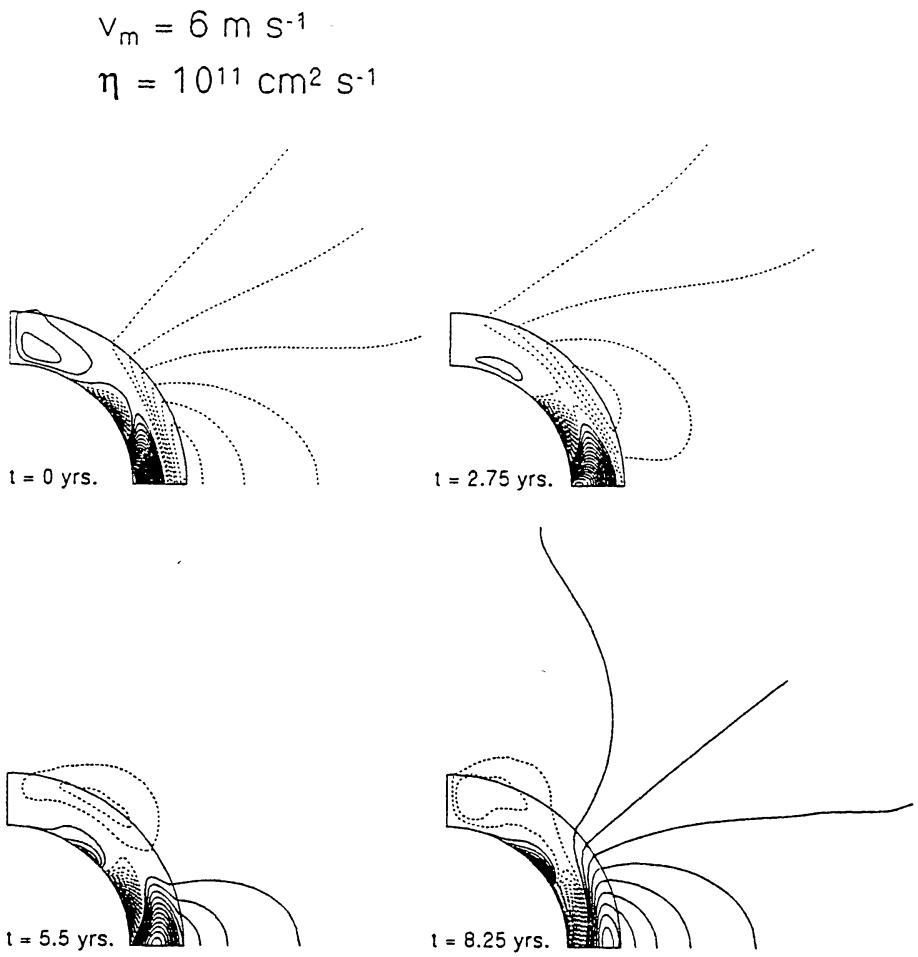

Fig. 2b. The snapshots of the evolving poloidal field lines at four successive epochs during a half of the solar cycle. The solid and dashed lines represent the regions of positive and negative A, respectively. We use a turbulent diffusion of 10^{11} cm^2 s^{-1} and the meridional flow pattern of Figure 2(a) with a maximum flow speed of 6 m s^{-1}.

Figure 2(c) with Figure 1 shows that the theoretical fit is reasonable. Figures 3(a–c) present the corresponding figures for the theoretical fit for negative α. A different meridional circulation (shown in Figure 3(a)) was chosen and δ was taken to be $5\pi/4$. Again a comparison of Figure 3(c) with Figure 1 shows the theoretical fit to be reasonable.

A detailed comparison of Figures 2(c) and 3(c) with Figure 1 shows that we are able to produce the correct tilt for the reverse butterfly pattern and the polar field changes sign at the time of solar maxima. Figure 1 shows some polar surges at the time of sunspot maxima, i.e., some tongues of opposite polarity extending to higher latitudes from the sunspot belts. These are not reproducecl in our model. Probably these surges are caused by flux coming from decaying active regions, although it is possible that they are due to the statistical fluctuations of the dynamo-generated field. Wang, Nash, and Sheeley (1989a) have made special efforts to model these polar surges. Our model, however, handles the high latitudes better than the model of the NRL group. It is seen in Figure 5(a) of Wang, Nash, and Sheeley (1989a) that

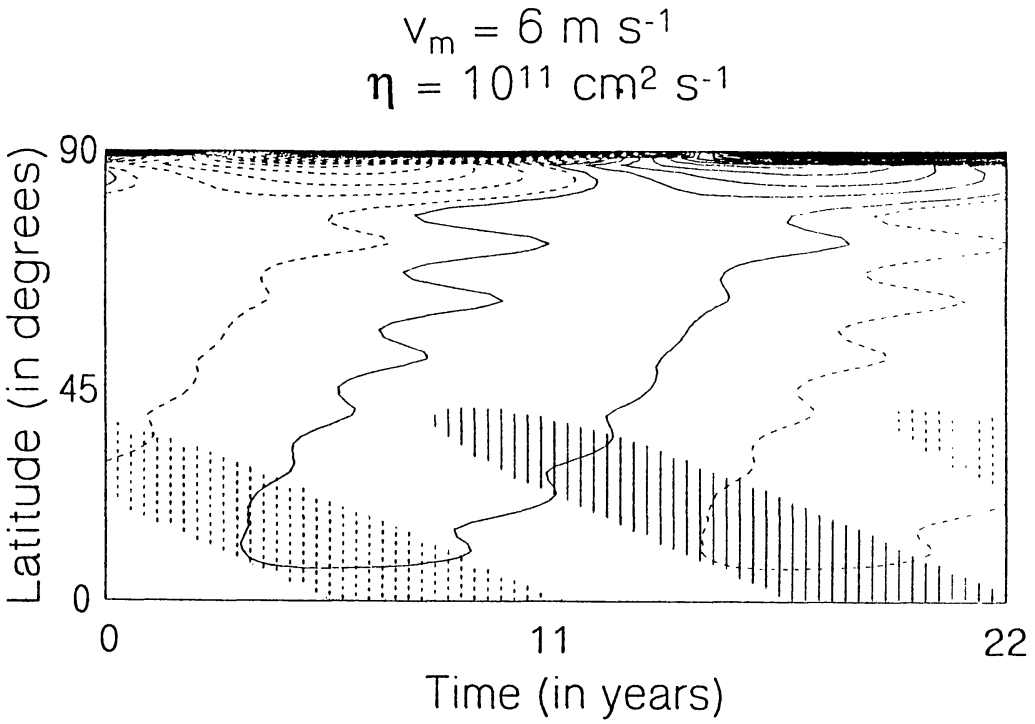

Fig. 2c. The theoretical latitude–time diagram for the photospheric radial fields (solid for positive and dashed for negative polarity) showing a 'reverse butterfly' pattern corresponding to Figure 2(b). A superimposed theoretical 'butterfly diagram' (solid and dashed shades implying positive and negative azimuthal fields respectively) for a positive α-effect in the northern hemisphere shows that the polar reversal is taking place at the beginning of sunspot maximum.

the magnetic field contours bend at high latitudes and tend to be horizontal. This is in contradiction with the observational data. We believe that we have been able to model the polar regions better, because we have a better representation of the flow at the polar regions where we allow the flow to sink underneath the surface, which is not the case with the model of the NRL group. The diffuse field evolves at the lower latitudes in a very different fashion and this is also not reproduced in our model. The low-latitude behavior and its significance is discussed at length in Section 4.

On comparing the figures for the two opposite signs of α, we find that a negative α would require a stronger upflow near the equatorial region (see Figure 3(a)) in order to match the observations. This is achieved by making the parameter β_2 larger so that the upflow is confined within a smaller horizontal extent and hence is stronger. Thus, as long as we do not know much about the meridional circulation underneath the solar surface, it is possible to fit observations with both signs of α by suitably adjusting the subsurface flow. The maximum values of the meridional flow at the surface are 6 and 7.7 m s^{-1} respectively in the two cases. These values are close to what has been used by the NRL group (Wang, Nash, and Sheeley, 1989a, b) and compare favorably with the observational estimate of Komm, Howard, and Harvey (1993) who report a maximum surface velocity of

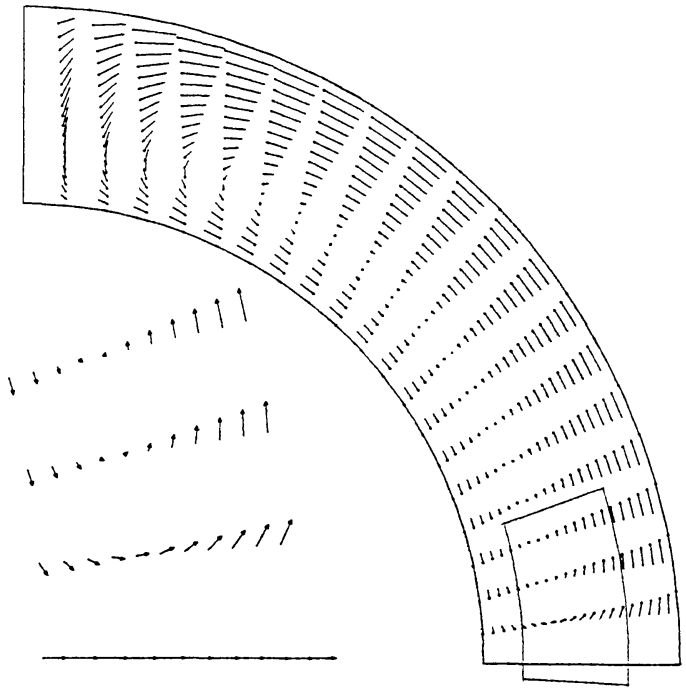

Fig. 3a. The meridional circulation pattern with a more concentrated flow (shown in enlarged form) at the equatorial region. Apart from β_2 being increased to $3k$, other parameters remain the same as in Figure 2(a).

13.2 m s^{-1}. The value of the meridional flow on the surface determines the tilts of the wings of reverse butterfly diagram and has to be in the range 5–10 m s^{-1} to fit the observations. It may be noted that Komm, Howard, and Harvey (1993) reported some variations of the meridional flow with the solar cycle and Wang, Nash, and Sheeley (1989a) found that the flow has to be made temporarily stronger to model the polar surges properly. We have so far carried on our calculations with time-independent meridional circulation. The values of the turbulent diffusion η used by us are, however, smaller than those used by the NRL group and smaller than what has been reported from surface observations (Schrijver and Martin, 1990). The significance of this is already discussed in Paper I.

Our model also opens up the possibility of studying the variation of the coronal shape with the solar cycle. In Figures 2(b) and 3(b), we see how the magnetic configurations of the corona change with the solar cycle. In the approach of Altschuler and Newkirk (1969), one component of the magnetic field on the solar surface (usually the line-of-sight component or the radial component) is taken as the boundary condition and the coronal field configuration is obtained from that. If the field above the photosphere is taken as a potential field, then specifying two components on the solar surface would overdetermine the problem and in general would not admit of solutions. In this approach, the field under the solar surface is not considered and hence the question of smoothly matching the field lines across the boundary does not arise. An attractive new feature of our model is that we solve for magnetic fields above and below the solar surface together self-consistently.

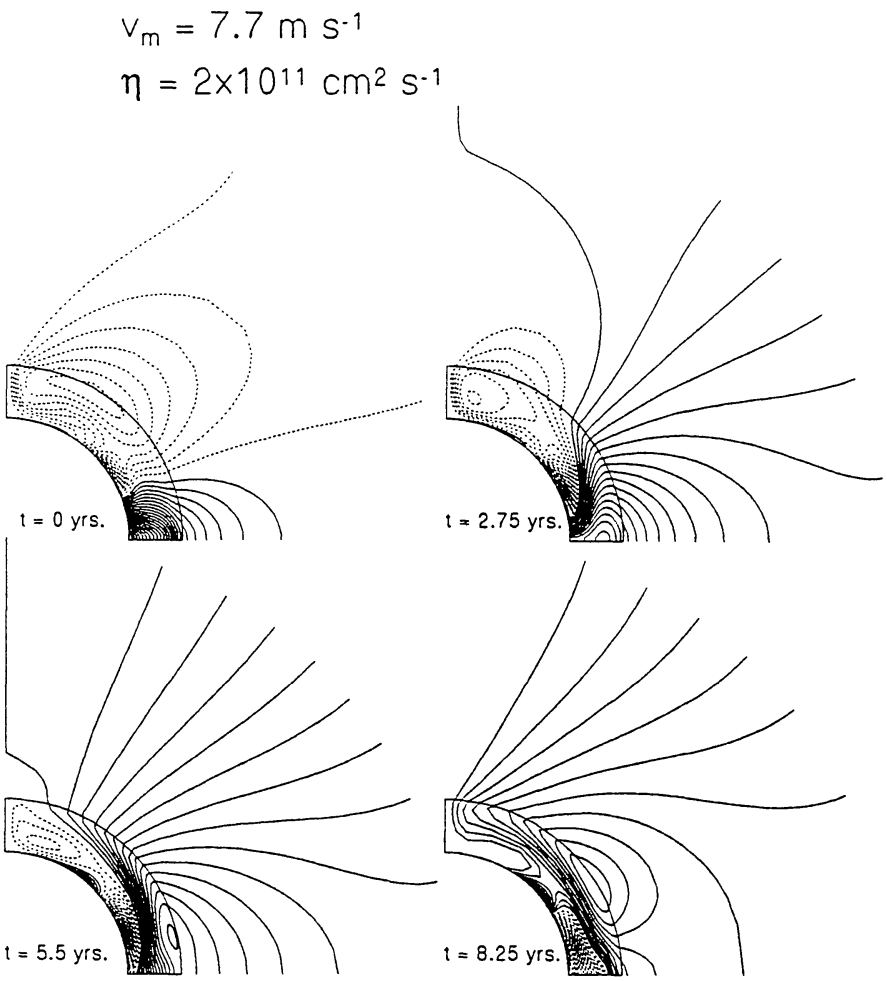

Fig. 3b. The snapshots of the evolving poloidal field lines (again solid and dashed representing positive and negative A regions, respectively) at four successive epochs during a half of the solar cycle. We use a diffusivity of 2×10^{11} cm^2 s^{-1} and the meridional fow pattern of Figure 3(a) with a maximum surface flow speed 7.7 m s^{-1}.

Hence the coronal field lines smoothly match the field lines inside the convection zone.

4. Conclusion

We have seen that the longitude-averaged observational data for the evolution of the large-scale diffuse field can be modelled theoretically by assuming the dynamo layer as the only source of the diffuse field. We are not suggesting that this is a faithful representation of everything that is happening inside the Sun. This work should be viewed more as a preparatory step towards more complete calculations in which the decay of active regions is taken as an additional source of the diffuse field. Since we have very little idea about the values of several crucial parameters, calculations with two sources open up too many possibilities and can give rise to wide varieties of solutions. A good understanding of the calculations presented

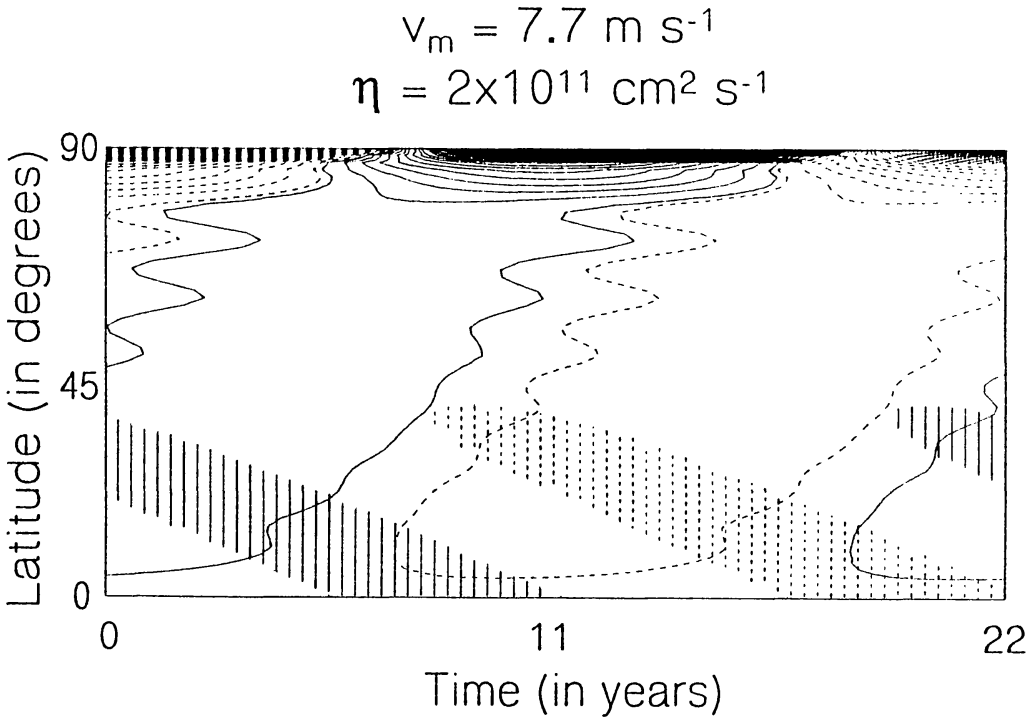

Fig. 3c. The theoretical latitude–time diagram for the photospheric radial fields (solid for positive and dashed for negative polarity) showing a 'reverse butterfly' pattern corresponding to Figure 3(b) and a superimposed theoretical 'butterfly diagram' (solid and dashed shades implying positive and negative azimuthal fields respectively) for a negative α-effect, clearly showing the polar reversal during the sunspot maximum.

in this paper would pave the way for understanding this more complex problem currently being investigated by us.

It is, however, not yet unambiguously clear whether active regions really make substantial contributions to the large-scale fields. Since active regions are usually widely separated on the solar surface, Parker (1984) pointed out that magnetic reconnection will not be very efficient for a global redistribution of flux around them and the most plausible route for the decay of active regions is that the flux is pulled down under the surface. Parker (1987) suggested that the same bundle of magnetic flux may emerge as active region and then be pulled down again and again, i.e., there may be efficient reprocessing of flux in the formation of successive active regions. If all the flux is produced by the dynamo in a thin layer, Parker (1987) argued that it is not possible to account for the total amount of flux seen on the surface unless we assume efficient reprocessing. If the magnetic field in the overshoot layer is much stronger than what was previously assumed (Schüssler, 1993), then this difficulty goes away and it is no longer essential to have efficient reprocessing of flux. However, the theoretical possibility still exists that most of flux emerging in the active regions is pulled below the surface rather than being spread around. Even if we take the extreme point of view that all the flux appearing in active regions sinks below without contributing to the large-scale field at all,

we have seen that still it is possible to model the longitude-averaged data for the large-scale diffuse field satisfactorily. We believe that this is an important point to note.

We have mainly focused on the distribution of the large-scale field in the higher latitudes appearing as a 'reverse butterfly' diagram in Figure 1. The distribution in the lower latitudes, however, appears dirferent. Stix (1976) noted that B_r and B_ϕ are completely out of phase in the lower latitudes and drift together towards the equator. This is seen in Figure 1 also. As pointed out by Stix (1976) and Schlichenmaier and Stix (1994), the observational difficulties in measuring mean B_r at lower latitudes are considerable and one should keep an open mind whether the data represent real observations. Granting that they are real, the fact that B_r and B_ϕ are out of phase (which means that B_ϕ and A are closer in phase) would imply a positive α (Stix, 1976). Since recent helioseismology observations would suggest a negative α for the dynamo layer at the bottom of the convection zone, Schlichenmaier and Stix (1994) investigate the question whether B_r and B_ϕ can be made out of phase in at least some parts of the dynamo layer even when α is negative.

We point out that there is a different way to solve the so-called 'phase dilemma'. We note that our theoretical Figures 2(c) and 3(c) do not reproduce these observations at the low latitudes which we are discussing. Most probably the diffuse field in the lower latitudes is dominated by contributions from the decay of the active regions and hence the present model without this contribution fails to match observations in the lower latitudes. If the production of a poloidal field from the decay of active regions (with the leading polarity closer to the equator) is described by a mean α-effect (although the mean field approximation may not be a very good approximation in this case), it is easy to see that this α must have a positive sign. Hence we should think in terms of an α-effect in the dynamo layer with a negative sign and an effective positive α to describe the decay of active regions higher up in the convection zone. In other words, the two sources of the diffuse field we are discussing must have α with different signs. An effective positive α near the solar surface would solve the 'phase dilemma' of Schlichenmaier and Stix (1994). If the diffuse field in the lower latitudes has a dominant contribution from the decay of active regions, then it is not difficult to understand why the diffuse fields there drift equatorward with the sunspots, as seen in Figure 7 of Stix (1976) and our Figure 1. Such a drift, however, would also follow if the data are not real and the concentrated leading polarity of active regions saturated the magnetograph more than the following polarity.

Why is the behavior of the diffuse field different in the lower latitudes from that in the higher latitudes (assuming the data for lower latitudes to be real)? We offer the hypothesis that lower latitudes are dominated by contributions from the decay of active regions, whereas the higher latitudes are dominated by diffuse fields which originated from the dynamo layer. Since the flux tubes giving rise to the active regions are believed to be anchored at the base of the convection zone

(Choudhuri, 1992; Moreno-Insertis, 1992), it is difficult to understand how the flux from decaying active regions can be freely carried to the higher latitudes and even to the poles. The flux from the decay of active regions presumably spreads in the surrounding regions in the neighborhood, unless it is pulled down completely as suggested by Parker (1984). Hence this component may dominate the observations of lower latitudes. But the higher latitudes should mainly have diffuse fields from the dynamo layer which do not have the same problem with the connectivity of field lines and hence can be transported to the poles without difficulty. One of the aims of our future calculations with two sources for the diffuse field is to validate these ideas.

Let us end with some comments on the point of view that there is no α-effect in the dynamo layer at all and the poloidal field results completely from the decay of active regions. The toroidal field in this scenario is still produced by the differential rotation at the base of convection zone where the poloidal field can be brought by meridional circulation. This possibility is currently being investigated by **B** (Durney, private communication). If this scenario were true, then the evolution of the large-scale field will have to be studied by taking the decay of active regions as the only source, and the dynamo source used in our calculations will have to be completely discarded. There are some obvious attractive features of this scenario. If the magnetic field at the base of the convection zone is much stronger than the equipartition value, then it is difficult to see how the traditional mean field α-effect may operate there, although the bouyancy-driven instabilities may be a way of giving rise to an effective α (Ferriz-Mas, Schmitt, and Schüssler, 1994). It would seem that taking the decay of active regions as the source of poloidal field is an attractive way of getting around this difficulty. However, the sign of α may pose a serious problem. Since we know very little about the conditions at the bottom of convection zone and even the buoyancy-driven instabilities do not suggest a definite sign of α (Ferriz-Mas, Schmitt, and Schüssler, 1993), one could take advantage of our ignorance and postulate a negative α to produce the equatorward drift of the dynamo wave. On the other hand, if we assume the α to be entirely due to the decay of active regions, then we run into the difficulty of having to build a model with both positive α and positive velocity shear, since both of these are now dictated by observations. There have been several calculations taking the α-effect and the differential rotation to be in different layers (see, for example, Moffatt, 1978, pp. 216–219), one of the latest being Parker's (1993) interface dynamo wave model. If diffusion is used to couple the layers, then one still has the same condition that the α-effect and the velocity shear have to have opposite signs in the northern hemisphere to produce an equatorward drift.

It remains to be seen if one can get around this constraint by using the meridional circulation in an essential way to bring the poloidal field from the top layer to the layer below. Unless the possibility of this is convincingly demonstrated, we have to assume a negative α at the base of the convection zone as the most likely possibility for the production of the poloidal field. As long as we nurture this point of view,

the base of the convection zone has to be regarded as a potential source for the large-scale magnetic field of the Sun.

Acknowledgements

We are most grateful to Dr R. Howard and Dr Y.-M. Wang for supplying us the data for sunspots and weak diffuse fields respectively. We wish to thank Drs. B. Durney, P. Hoyng, M. Schüssler and M. Stix for stimulating discussions. We also thank the Supercomputing Education and Research Centre and the Distributive Information Centre of Indian Institute of Science for the use of their computing and graphics facilities. M.D. would like to thank Council of Scientific and Industrial Research for financial support through the Award No. 9/79(248)/89-EMRI. A.R.C.'s stay at the Kiepenheuer Institute was made possible by a Fellowship from the Alexander von Humboldt Foundation.

Appendix. The Phase Relation between the Toroidal and Poloidal Components

To find the phase relation between the toroidal and poloidal components for a plane dynamo wave, we assume a rectangular geometry appropriate for the northern hemisphere, with x corresponding to the vertical direction, y to the azimuthal direction, and z to the longitudinal direction (i.e., the equatorward propagation of the dynamo wave will mean propagation in negative z direction). For an $\alpha^2\omega$ dynamo, we have a pair of equations (see Choudhuri, 1990):

$$\left(\frac{\partial}{\partial t} - \eta\nabla^2\right) B_y = -G\frac{\partial A_y}{\partial z} - \alpha\nabla^2 A_y \,, \tag{15}$$

$$\left(\frac{\partial}{\partial t} - \eta\nabla^2\right) A_y = \alpha B_y \,. \tag{16}$$

To obtain the necessay phase relations, we try solutions of the type

$$A_y = \hat{A} e^{i(\omega t + k_x x + k_z z)} \,, \tag{17}$$

$$B_y = \hat{B} e^{i(\omega t + k_x x + k_z z + \delta)} \,, \tag{18}$$

where $\hat{A}$, $\hat{B}$, δ, ω, k_x, k_z are all assumed to be real. We would further take $\hat{A}$ and $\hat{B}$ to be positive. For the equatorward propagation (i.e., in the negative z direction) of the dynamo wave, ω and k_z will have to be of the same sign. We would take them also to be positive. Substituting (17) and (18) in (15) and (16), we have

$$(i\omega + \eta K^2)\hat{B} e^{i\delta} = (-ik_z G + \alpha K^2)\hat{A} \,, \tag{19}$$

$$(i\omega + \eta K^2)\hat{A} = \alpha \hat{B} e^{i\delta} \,, \tag{20}$$

where

$$K^2 = k_x^2 + k_z^2 \,.$$

It is easy to see that (19) and (20) lead to the following real equations:

$$\eta^2 K^2 - \omega^2 = \alpha^2 K^2 \,, \tag{21}$$

$$2\omega\eta K^2 = -\alpha G k_z \,. \tag{22}$$

For equatorward propagation (i.e., for the same sign of ω and k_z), it is easy to see from (22) that αG has to be negative. There are two possibilities: (i) α positive and G negative; (ii) α negative and G positive. In the first case, we find from (20) and (21) that (keeping in mind that ω, $\hat{A}$, $\hat{B}$ are positive)

$$\delta = \tan^{-1} \frac{1}{\sqrt{1 + \left(\dfrac{\alpha K}{\omega}\right)^2}} \,. \tag{9}$$

On the other hand, in the second case, we would have

$$\delta = \pi + \tan^{-1} \frac{1}{\sqrt{1 + \left(\dfrac{\alpha K}{\omega}\right)^2}} \,. \tag{10}$$

It is interesting to consider now the two limits of $\alpha\omega$ and ω^2 dynamos. For an $\alpha\omega$ dynamo, we have $(\alpha K/\omega)^2$ equal to zero (see Choudhuri, 1990) so that δ is $\pi/4$ in the first case (i.e., positive α case) and $5\pi/4$ in the second case (i.e., negative α case). For an α^2 dynamo, $(\alpha K/\omega)^2$ is infinite so that δ in these two cases turns out to be 0 and π.

References

Altschuler, M. D. and Newkirk, G. W.: 1969, *Solar Phys.* **9**, 131.
Babcock, H. D.: 1959, *Astrophys. J.* **130**, 364.
Bumba, V. and Howard, R.: 1965, *Astrophys. J.* **141**, 1502.
Caligari, P., Moreno-Insertis, F., and Schüssler, M.: 1994, *Astrophys. J.* **441**, 886.
Choudhuri, A. R.: 1989, *Solar Phys.* **123**, 217.
Choudhuri, A. R.: 1990, *Astrophys. J.* **355**, 733.
Choudhuri, A. R.: 1992a, *Astron. Astrophys.* **253**, 277.
Choudhuri, A. R.: 1992b, in J. H. Thomas and N. O. Weiss (eds.), *Sunspots: Theory and Observations*, Kluwer Academic Publishers, Dordrecht, Holland, p. 243.
Choudhuri, A. R. and Gilman, P. A.: 1987, *Astrophys. J.* **316**, 788.
D'Silva, S.: 1993, *Astrophys. J.* **407**, 385.

D'Silva, S. and Choudhuri, A. R.: 1993, *Astron. Astrophys.* **272**, 621.
DeVore, C. R. and Sheeley, N. R.: 1987, *Solar Phys.* **108**, 47.
DeVore, C. R., Sheeley, N. R., and Boris, J. P.: 1984, *Solar Phys.* **92**, 1.
Dikpati, M. and Choudhuri, A. R.: 1994, *Astron. Astrophys.* **291**, 975 (Paper I).
Fan, Y., Fisher, G. H., and DeLuca, E. E.: 1993, *Astrophys. J.* **405**, 390.
Ferriz-Mas, A., Schmitt, D., and Schüssler, M.: 1994, *Astron. Astrophys.* **289**, 949.
Howard, R. and LaBonte, B. J.: 1981, *Solar Phys.* **74**, 131.
Komm, R. W., Howard, R. F., and Harvey, J. W.: 1993, *Solar Phys.* **147**, 207.
Leighton, R. B.: 1964, *Astrophys. J.* **140**, 1547.
Makarov, V. I. and Sivaraman, K. R.: 1989, *Solar Phys.* **119**, 35.
Makarov, V. I., Fatianov, M. P., and Sivaraman, K. R.: 1983, *Solar Phys.* **85**, 215.
Moffatt, H. K.: 1978, *Magnetic Field Generation in Electrically Conducting Fluids*, Cambridge University Press, Cambridge.
Moreno-Insertis, F.: 1992, in J. H. Thomas and N. O. Weiss (eds.), *Sunspots: Theory and Observations*, Kluwer Academic Publishers, Dordrecht, Holland, p. 385.
Parker, E. N.: 1979, *Cosmical Magnetic Fields*, Clarendon Press, Oxford.
Parker, E. N.: 1984, *Astrophys. J.* **281**, 839.
Parker, E. N.: 1987, *Astrophys. J.* **312**, 868.
Parker, E. N.: 1993, *Astrophys. J.* **408**, 707.
Petrovay, K. and Szakály, G.: 1993, *Astrophys. J.* **274**, 543.
Schlichenmaier, R. and Stix, M.: 1995, *Astron. Astrophys.* (in press).
Schrijver, C. J. and Martin, S. F.: 1990, *Solar Phys.* **129**, 95.
Schüssler, M.: 1993, in F. Krause, K.-H. Rädler, and G. Rüdiger (eds.), 'The Cosmic Dynamo', *IAU Symp.* **157**, 27.
Sheeley, N. R., DeVore, C. R., and Boris, J. P.: 1985, *Solar Phys.* **98**, 219.
Sheeley, N. R., Wang, Y.-M., and Harvey, J. W.: 1989, *Solar Phys.* **119**, 323.
Stenflo, J. O.: 1992, in K. L. Harvey (ed.), *The Solar Cycle*, ASP Conf. Series 27, p. 83.
Stix, M.: 1976, *Astron. Astrophys.* **47**, 243.
van Ballegooijen, A. A. and Choudhuri, A. R.: 1988, *Astrophys. J.* **333**, 965.
Wang, Y.-M. and Sheeley, N. R.: 1991, *Astrophys. J.* **375**, 761.
Wang, Y.-M., Nash, A. G., and Sheeley, N. R.: 1989a, *Astrophys. J.* **347**, 529.
Wang, Y.-M., Nash, A. G., and Sheeley, N. R.: 1989b, *Science* **245**, 712.